Original Research Article

Charge Transport Enhancement in Anthracene Molecular Junction: DFT Studies

ABSTRACT

Device miniaturization and a desire to add some functionality for the next-generation electronic circuits have prompted the research community into a single molecule electronics. Here, we analyzed anthracene molecules coupled to Au electrodes through anchor groups. By using density functional theorem (DFT) in combination with non-equilibrium Green's functional (NEGF) formalism, we investigated the frontier molecular orbitals (MOs) and charge transport nature of the junction by giving special consideration to the anchoring groups (NH_2, S, CN and SH), chemical impurity doping (B, N and NB) and side groups ($-CH_3$, $-NH_2$, and $-NO_2$). The results shows that the MOs can vary depending upon the substituents or dopants used. NB-doped has the lowest HOMO-LUMO gap and is expected to be more stable. We also observed that charge transport can be p-type or n-type depending on the anchor materials used. It is found that the amines anchor group have a higher conductance for an anthracene molecular junctions (MJs). These findings can be very helpful in understanding and fabrication of either n-type or p-typed high conductive single molecule electronic components.

Keywords: *Anthracene, Charge transport, DFT, HOMO-LUMO, NEGF, Transmission*

1. INTRODUCTION

Increasing demands for power consumption and area reduction and improvement in switching speed of electronic devices have prompted the research community to search for next-generation technologies that can replace conventional silicon semiconductor technology. Molecular electronics is one of such technology that can enable high integration densities and low power consumption [1]. The ultimate goals of molecular electronics are the miniaturization of electronic devices and the integration of functional molecular devices into the circuits.

Charge transport in molecular nanostructures is a very active field of experimental and theoretical research, which has seen considerable progress in recent years, and according to Michael and Ferdinand [2], the most widely studied architecture in this field is a molecular junction (MJ), where a single molecule is bound to metal or semiconductor electrodes clusters. MJs are also referred to as "Metal-molecule-metal (M-m-M) junction". Figure 1, illustrate the anthracene single molecule junction, where the molecule is connected to two electrodes via amines anchoring group. MJs combine the possibility to study the fundamental aspects of non-equilibrium many-body quantum physics at the nano-scale with the perspective for technological applications in molecular nano-electronic devices.

The development of theoretical and experimental techniques made it possible to measure thermoelectric properties at single molecule level. Providing new insight into different aspects of structure-function relationship in single-molecule junction [3]. Many techniques such as scanning tunneling microscope break junction (STM-BJ), mechanically controllable break junction (MCBJ) and electro-migrated break junction (EMBJ) were developed to measure the thermopower and electrical conductance of single molecule junctions [4-6]. Also, conductive atomic force microscope (C-AFM) technique was used by Tan and co-workers [7], for thermal conductance measurements in networks of MJs featuring multiple molecules. Widawsky *et al.,*[8], was able to measure the conductance in single-molecule junction via direct measurement of electrical current under zero bias using STM-BJ based technique.

The electric and thermoelectric properties of single-molecule junction can be modified by manipulating their transport properties which is explored by theoretical and experimental studies. For instance, changing the molecule-electrode coupling geometry [9], chemical doping of the molecule [10], or even functionalization of the molecule with side-group [11], can substantially modify the conductance in MJs. More effectively, structural or chemical modification of anchoring group [12,13] can significantly tune the electric properties of MJs.

In this work, we investigated the charge transport in an anthracene-based MJ by considering four different anchoring groups, three different side-groups and three doping procedures independently.

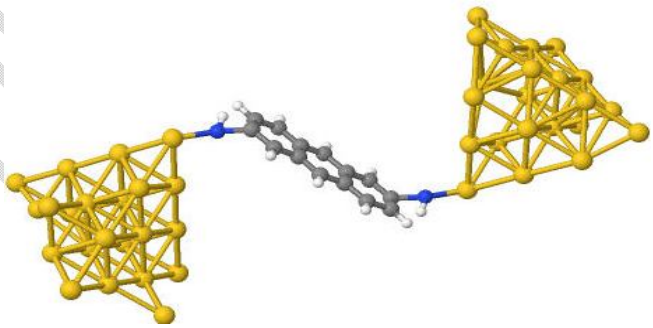

Figure 1: Anthracene molecular junction connected to Au(111) electrodes via Amines anchoring group.

2. METHOD

We investigated the electrical properties such as the frontier molecular orbital (HOMO and LUMO), the transmission coefficients T(E) and the conductance (G) which is the ability of an electron to transmit or

pass through an anthracene MJ. After forming the junction, we calculated these properties in three different phases. In the first phase, we investigated the effects of an anchoring group, and we used four different groups which are amines (-NH_2), cyanides (-CN), sulphur (-S) and thiol (-SH) groups. For the second phase of this work, we used methyl (-CH_3), amine (-NH_2) and nitro (-NO_2) as three different side groups but maintaining the same anchor group. The last phase of this work is chemical doping, where we used N and B, as our dopant since they are both the most commonly used dopants for carbon-based materials [11]. Throughout the work we maintained Au(111) as our source and drained electrodes.

The calculations were performed using density functional theorem (DFT) and non-equilibrium Green's function (NEGF) formalism. The electronic structure calculations were carried out via DFT as implemented in the FHI-aims computer code [14], with the Perdew-Burke-Ernzerhof (PBE), while the transport properties of the system were calculated using NEGF approach as implemented in the Aitranss computer code [15-17].

The exchange and correlation interaction energies of electrons are described by functional Perdew-Zunger local density approximation (LDA). DFT is based on quite a rigid conceptual frame work. For many-body problem, the Schrondinger equation becomes

$$\left[\sum_i^N \left(\frac{-\hbar^2\nabla_i^2}{2m} + V(r_i)\right) + \sum_{i<j} U(r_i, r_j)\right]\Psi(r_1, r_2, .., r_N) = E\Psi(r_1, r_2, .., r_N) \qquad (1)$$

Where N is number of electrons and $U(r_i, r_j)$ is the electron-electron interaction.

The transport properties of the structures are calculated via the Landauer-Buttiker formalism defined by the Green's function in equation (2).

$$G(E) = [ES - H_C - \sum_L(E) - \sum_R E]^{-1} \qquad (2)$$

Where E is the energy, H_c is the Hamiltonian, and S is the overlap matrix corresponding to the scattering region, while $\sum_{L/R}(E)$ are the self-energies of the left and right electrodes. The transmission coefficients are calculated after achieving self-consistency in the Green's function calculation as

$$T(E) = T_r[G(E)\Gamma_L(E)G(E)^{\dagger}\Gamma_R(E)] \qquad (3)$$

With $\Gamma_{L/R}(E) = i\left(\sum_{L/R} E - \sum_{L/R}(E)^{\dagger}\right)$, where Γ_L and Γ_R are the coupling functions. The transmission coefficient T(E) gives the transmission probability of electron having a certain energy E.

The electrical conductance is related to the transmission coefficient through the Landauer formular

$$G = \left(\frac{2e^2}{h}\right) \int_{-\infty}^{\infty} T(E) \left(\frac{\partial f(E,T)}{\partial E}\right) dE \qquad (4)$$

Where $f(E,T)$ is the distribution function given as $f(E,T) = \left[e^{(E-E_f)/k_BT} + 1\right]^{-1}$ with k_B a Boltzmann's constant and E_f is the Fermi energy of the electrodes.

3. RESULTS

We first reported the effects of an anchoring group on the junction, then followed by that of molecular impurity doping and side groups respectively.

3.1 Anchoring materials: Here, the anthracene molecule is coupled to the Au- electrodes via different anchoring groups. The choice of anchoring groups can determines the nature of transport in the MJ to be either p-type (HOMO-dominated) or n-type (LUMO-dominated). Molecular self-consistent Hamiltonian (MPSH) for frontier molecular orbitals are shown in Fig 2. It can be seen that in (a), the HOMO for pristine (-H) is localized within the anthracene molecule, while the LUMO is delocalized. The cyanide (CN) group substituent has negligible impact on both HOMO and LUMO as they almost remains similar to that of pristine case. Both cyanide and thiol reduces the HOMO-LUMO gap to 2.15eV and 2.08eV respectively. Sulphide anchoring group on the other hand has the most physical impact on the HOMO, but has the same influence on the LUMO as the amines (NH_2). As it can be seen from Figure 2e, the HOMO is highly localized on the sulphur atoms, but not within the anthracene molecule. Thus, electrons cannot easily pass through the molecule. Even though sulphur has the ability to converge HOMO-LUMO gap to a minimum of 0.43eV from the initial 2.32eV (see table 1), it cannot be chosen as a good anchor group for electron transport applications. Amines on the other hand has little impact on both the HOMO and the LUMO structures, but it reduces the HOMO-LUMO gap to 1.40eV. Amines should be regarded as the best anchor for an anthracene-based MJ. As for the thiol, it delocalized the HOMO, but has little impact on the LUMO as it remains delocalized as in the case of pristine.

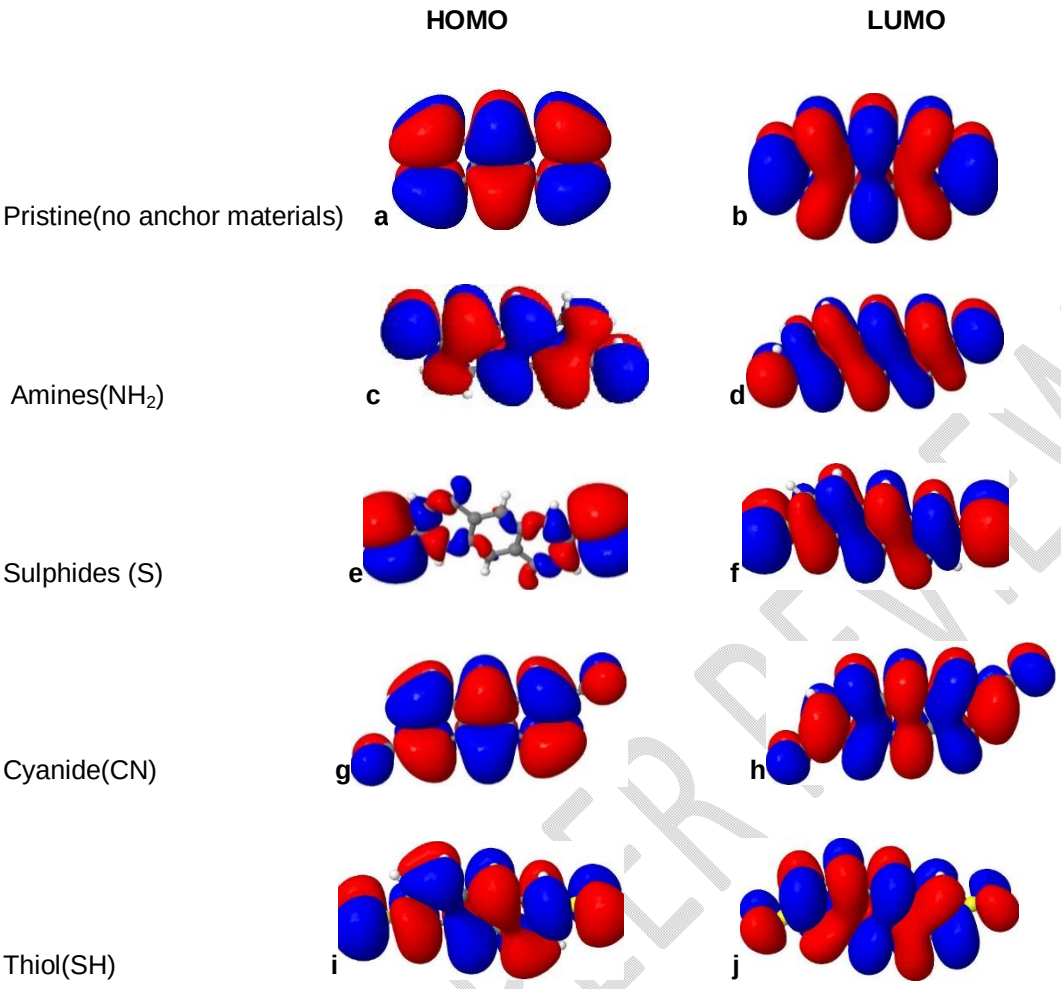

Figure 2: Frontier orbitals changes, due to the introduction and changing the anchor materials

Table 1: HOMO and LUMO variation with different anchor groups

Anchor material	HOMO (eV)	LUMO (eV)	HOMO-LUMO gap(eV)
Pristine (H)	-5.03	-2.71	2.32
Amines (NH_2)	-5.47	-4.07	1.40
Cyanides (CN)	-5.99	-3.84	2.15
Sulphur (S)	-5.36	-4.93	0.43
Thiol (SH)	-4.87	-2.79	2.08

Figure 3 shows that, amines (purple), and sulphur (blue) has minimum HOMO-LUMO gap, but the former possess the highest transmission coefficient, T(E), at Fermi energy which valued to 0.975 units. This means that, considering equation 3, it has a higher conductance, G, than sulphur, thiol (magenta) and cyanides (green), which has transmissions of 0.939, 0.872 and 0.711 respectively. The HOMO level of thiol is closer to E_F, and thus indicated that it gains a partial electrons from Au atom in the electrodes.

Thus, it is a p-type (HOMO-dominated) transport. Whereas, amines and cyanides has an n-type (LUMO-dominated) transport since their LUMO energy levels remains closer to E_F.

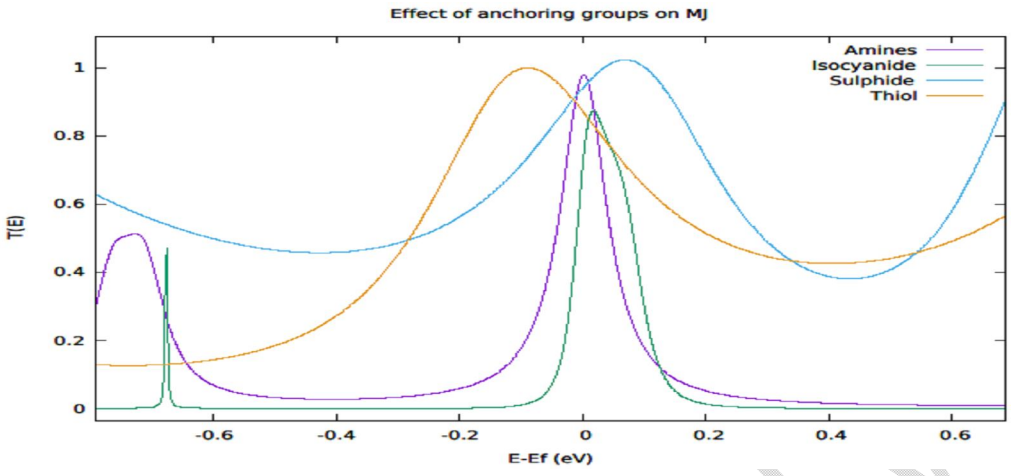

Figure 3: Transmission coefficients of different anchoring-group versus energy.

These results are in total agreements with the previous work by Balachandran, *et al.,* (2012).

3.2 Doping: we consider a single carbon substitution by B and N, and a double carbon substitutions by N and B atoms at the edge of the middle benzene ring of the simple geometry of an anthracene (scattering region) MJ. For all the configurations, we maintained amines as our anchor group. From the calculated frontier molecular orbitals (Figure 4), we found that the HOMO is localized on the donor anthracene (ie B-atom), but the LUMO is delocalized. This indicated that, the electron transmission takes place through the doping site of the molecule. The HOMO is partially localized on N-doped anthracene, while LUMO does not. For the case of NB-doped molecule, both HOMO and LUMO are delocalized and it indicated that the transmission may take place from both sides of the molecule.

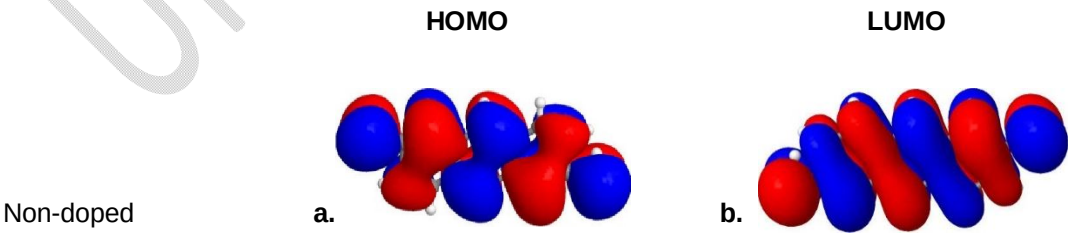

B-doped c. 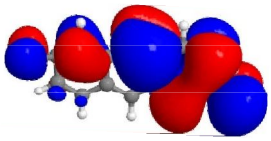 d. 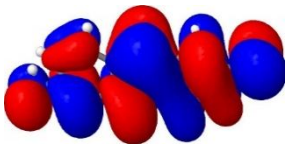

N-doped e. 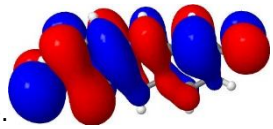 f. 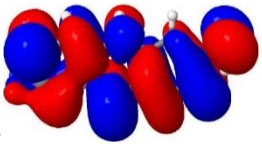

NB-doped g. 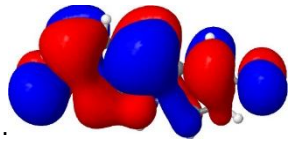 h. 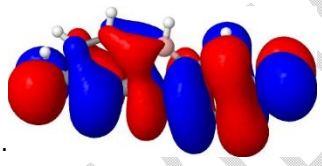

Figure 4: Frontier molecular orbitals for doped and non-doped anthracene

Table 2, shows that impurity doping affects the HOMO-LUMO gap of the scattering region of anthracene MJ. Even though it increases the value of HOMO energy level to -5.33eV, the B-doping process converged HOMO-LUMO gap to 1.42eV, by further increasing the value of LUMO to -3.91eV from initial -4.07eV in table 1. Table for N-doped anthracene, the HOMO-LUMO gap is converged to 0.97eV. While the excitation will becomes easier for NB-doped anthracene because it has the lowest HOMO-LUMO gap of 0.25eV. It increases the HOMO energy level to -4.88eV, and becoming the most stable among others. This result is in agreement with the previous works [18,19].

Table 2: HOMO-LUMO variation with impurity doping

Doping	HOMO (eV)	LUMO (eV)	HOMO-LUMO gap(eV)
B-doped	-5.33	-3.91	1.42
N-doped	-4.27	-3.30	0.97
NB-doped	-4.88	-4.63	0.25

Figure 5, shows that, NB-doped anthracene MJ has the highest value of conductance since it has the highest value of transmission coefficient T(E), at Fermi energy. Its HOMO is the closest energy level to E_F, hence it is a p-type (HOMO-dominated) transport. The B- and N-doped anthracene MJs has the least values of transmission coefficients T(E) of 0.54 and 0.39 units respectively. For B-doped anthracene the LUMO is the closest energy level to E_F. This also shows that B-doping shift the LUMO towards the Fermi energy, while the N-doped molecule shifts the HOMO level towards the Fermi energy level. When the MJ is doped with NB, the HOMO-LUMO gap is reduced slightly, but there is a significant increase in

transmission coefficient when compared to N- and B-doped. When carbon atoms are replaced by B, N or NB atoms, the electronic structure can be modified. The shift of the HOMO-LUMO gap can be described by the effect of p-type and n-type impurities on the B-, N- or NB-doped anthracene molecule. Since B is an electron-donating impurity, it increases the energy of the system because it shifts the LUMO level close to the Fermi energy level hence it is n-type transport. In contrast, for electron-withdrawing, N-doping electron transport occurs through HOMO and the HOMO-LUMO gap shifts to the left side of the Fermi energy and it is p-type transport.

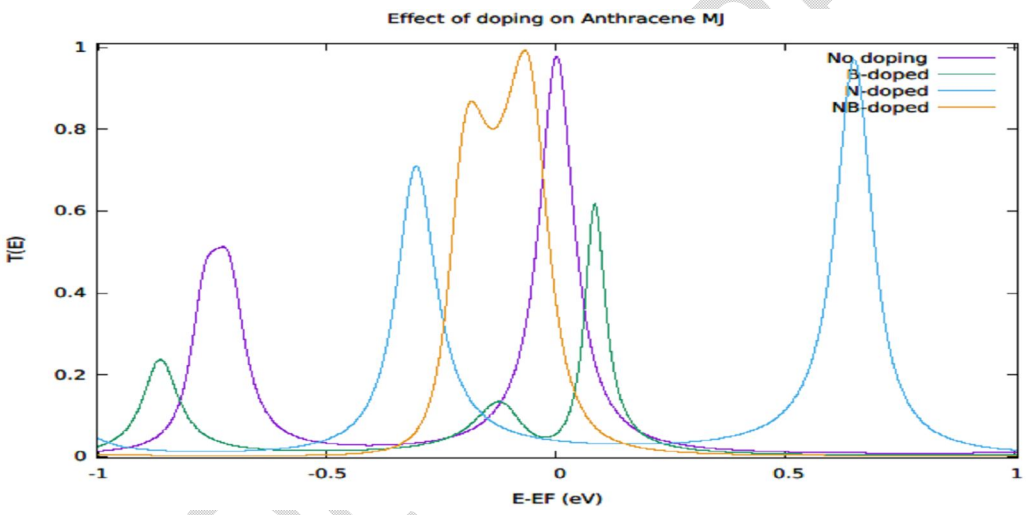

Figure 5: Transmission coefficients of B-doped, N-doped and NB-doped anthracene MJ

3.3 Side Group: So far, we discussed about the effects of four different anchoring groups and three impurity doping. We now look at the three different side groups i.e amine ($-NH_2$), nitro ($-NO_2$) and methyl ($-CH_3$) connected on the central benzene ring of the anthracene MJ. Introduction of side group can regulate HOMO or LUMO alignment, and the nature of transport depending on the nature of the side group (donating or accepting).

The calculated frontier orbitals indicated that, HOMO and LUMO energy states are anti-symmetric in the plane of the anthracene molecule. This indicates that they represent the π-orbitals on each carbon atom perpendicular to the plane of the molecule. The HOMO is localized for the methyl and amine side group due to their electron donating nature. On the other hand, for the case of an electron-accepting side group (i.e nitro) LUMO is localized.

Figure 6, represents the impacts of side groups on the HOMO and LUMO of an anthracene molecule coupled to Au electrodes via amines anchor group. The introduction of the side groups changes the nature of both the HOMO and LUMO of the anthracene molecule. For all of these three cases (i.e CH_3 NH_2 and NO_2) the frontier molecular orbitals are delocalized throughout the molecule, and hence the transmission can take place at both side of the molecule.

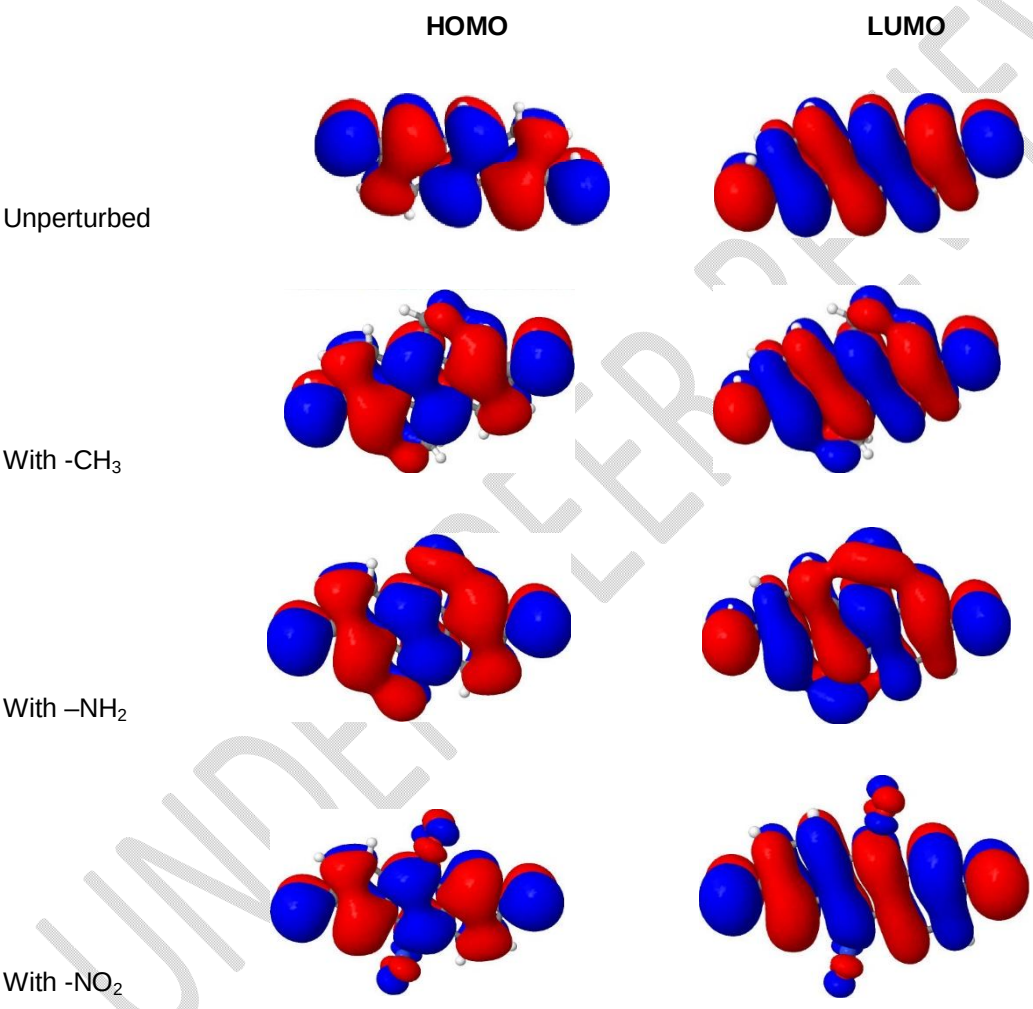

Figure 6: Frontier molecular orbitals for different side groups

Looking at the table 3, we observed that both of side groups converges the HOMO-LUMO gap compared to the unperturbed molecule. They both have similar impact on the molecule.the HOMO-LUMO gaps for an anthracene with $-CH_3$, $-NH_2$ and $–NO_2$ side groups are 1.41eV, 1.42eV and 1.38eV respectively. This shows that Nitro ($-NH_2$) is more stable and excites easily compared to the other two.

Table 3: HOMO and LUMO variations with different side groups

Side group	HOMO (eV)	LUMO (eV)	HOMO-LUMO gap (eV)
Methyl (-CH_3)	-5.34	-3.93	1.41
Amines (-NH_2)	-5.02	-3.60	1.42
Nitro (-NO_2)	-6.19	-4.81	1.38

Figure 7, shows the transmission coefficient against energy for the three side groups attached and the unpertubed (without side group) anthracene MJ. It is indicated that the introduction of the side groups can shift the location of the transmission picks or even modulated their shape. It can be seen that methyl side group has a very minimal effect on the transmission curve. The amine (blue) side group shifted the transmission pick to the right of E_F, making it a LUMO-dominated (n-type) transport. On the contrary, the nitro (magenta) is an electron-accepting side-group, it shifts the transmission coefficient to the left side of the Fermi energy. It showed a HOMO-dominated transmission. This is in agreement with the previous works [11, 20].

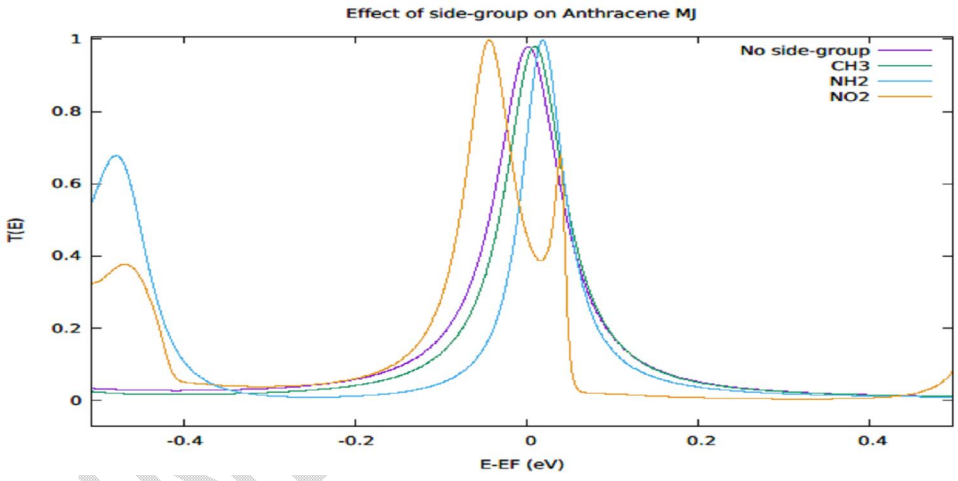

Figure 7: Transmission coefficient of different side-groups and their effects on molecular junction

4. CONCLUSION

We have employed DFT calculations in combination with NEGF formalism and theoretically analyzed the electronic transportations properties with emphasis on electrical conduction. We first investigated the amines (NH_2), sulphide (S), cyanide (CN) and thiol (SH) anchoring groups. We focused on how those

anchoring groups modifies the functionality of anthracene single molecule junction when connected to gold electrodes via each and every one of them. The results shows that, in thiol (SH) and amines (NH_2) anchoring groups, the HOMO picks are closer to the Fermi energy level, making it a HOMO-dominated transport, whereas in cyanides (CN) and sulphide (S) anchor groups, the LUMO picks are closer to Fermi energy level, making it a LUMO-dominated transport.

We also investigated the effects of impurity doping on the anthracene molecule where we used B and N as our chemical dopants. B-doped shifts the HOMO level close to the Fermi energy level hence it is p-type transport, while N-doping electron transport occurs through LUMO and shifts to the left side of the Fermi energy and it is n-type transport.

Lastly, we maintained the amine anchoring group and investigated the effects of amine ($-NH_2$), nitro ($-NO_2$) and methyl ($-CH_3$) side-groups. The results shows that amine side group shifted the transmission pick to the left of E_F, making it a HOMO-dominated (n-type) transport, but the nitro side group, being an electron-accepting side-group, it shifts the transmission coefficient to the left side of the Fermi energy, and showed a LUMO-dominated transmission. While the methyl (CH_3) side group, has negligible effect on the transport.

References

[1] Sirohi A, SanthiBhushan B, Srivastava A. Charge transport in polythiophene device: DFT analysis. Journal of Molecular Modelling, 2021, 77, 1-10.

[2] Michael T, Ferdinand E. Perspective: Theory of quantum transport in molecular junctions. THE JOURNAL OF CHEMICAL PHYSICS, 2018, 148, 1-16.

[3] Wang K, Meyhofer F, Reddy P. Thermal and thermoelectric properties of molecular junctions. Adv. Funct. Mater, 2020, 30, 1904534.

[4] Reddy P, Jang S–Y, Segalman RA, Majumdar A. (2007). Thermoelectricity in molecular junctions. Science, 2007, 315, 1568-1571.

[5] Torres A, Pontes RB, da Silva AJ, Fazzio A. Tuning the thermoelectric properties of a single molecule junction by mechanical stretching. Phys. Chem. Chem. Phys., 2015, 17, 5386-5392.

[6] Kim Y, Jeong, W, Kim K, Lee W, Reddy P. Electrostatic control of thermoelectricity in molecular junctions. Nat. Nanotechnol. 2014, I9, 881.

[7] Tan A, Sadat S, Reddy P. Measurement of thermopower and current-voltage characteristics of molecular junctions to identify orbital alignment. Appl. Phys. Lett. 2010, 96, 013110.

[8] Widawsky JR, Darancet P, Neaton JB, Venkataraman L. Simultaneous determination of conductance and thermopower of single molecule junctions. Nano Lett. 2012, 12, 354-358.

[9] Akbarabadi RS, Rahimpour SH, Bagheri TM, Golsanamlou Z. Impact of coupling geometry on thermoelectric properties of oligophenyl-base transistor. Chin. Phys. B., 2017, 26, 027303.

[10] Golsanamlou Z, Bagheri TM, Rahimpour SH. Improvement of thermoelectric efficiency of the polyaniline molecular junction by the doping process. Phys. Chem. Chem. Phys., 2015, 17, 13466-13471.

[11] Akbarabadi RS, Rahimpour SH, Tagani MB. Side-group-mediated thermoelectric properties of anthracene single-molecule junction with anchoring groups. Scientific Reports, 2021, 11, 8958. https://doi.org/10.1038/s41598-021-88297-2.

[12] Noori MD, Sangtarash S, Sadeghi H. The effect of anchor group on the phonon thermal conductance of single molecule junctions. Appl. Sci. 2021, 11, 1066.

[13] Zhao X, Stadler R. DFT-based study of electron transport through ferrocene compounds with different anchor groups in different adsorption configurations of stm setup. Phys. Rev. B. 2019, 99, 045431.

[14] Blum V, Gehrke R, Hanke F, Havu P, Havu V, Ren X, Reuter MS. Ab initio molecular simulations with numeric atom-centered orbitals. Computer Physics Communications, 2009, 2175-2196.

[15] Arnold A, Weigend F, and Evers F. Quantum chemistry calculations for molecules coupled to reservoirs: Formalism, implementation, and application to benzenedithiol. The Journal of Chemical Physics. 2007, 174101-12.

[16] Wilhelm J, Walz M, Stendel M, Bagrets A, Evers F. Ab initio simulations of scanning-tunneling-microscope images with embedding techniques and application to C58-dimers on Au(111). Phys. Chem. Chem. Phys., 2013, 6684-6690.

[17] Bagrets A. Spin-polarized electron transport across metal-organic molecules: a density functional theory approach. *Journal of Chemical Theory and Computation,* 2013, 2801-45.

[18] Akbarabadi RS, Rahimpour SH, Bagheri TM, Golsanamlou Z, Tagani MB. Enhanced thermoelectric properties in anthracene molecular device with graphene electrodes: the role of phononic thermal conductance. Scientific Reports, 2020, 10, 10922. https://doi.org/10.038/s41598-020-67964-w.

[19] Blanca B, Blasé X, Francois T, Stephan R. Anomalous Doping Effects on Charge Transport in Graphene Nanoribbons. Physical Review Letters, 2009, 102, 9, 096803. DOI: 10.1103/PhysRevLett.102.096803**.**

[20] Li B, Ji X, Tian L, et al. Sequence modulation of tunneling barrier and charge transport across histidine doped oligo-alanine molecular junction. Chin. Chem. Lett. 2021. https://doi.org/10.1016/j.cclet.2021.04.013.